2015 European Control Conference (ECC)
July 15-17, 2015. Linz, Austria

Simultaneous Localization and Mapping in Sensor Networks: a GES sensor-based filter with moving object tracking

Pedro Lourenço, Pedro Batista, Paulo Oliveira, and Carlos Silvestre

Abstract— **This paper presents the design, analysis, and validation of a globally exponentially stable (GES) filter for tridimensional (3-D) range-only simultaneous localization and mapping in sensor networks with moving object tracking. For observability analysis purposes, two nonlinear sensor-based dynamic systems are formulated resorting only to exact linear and angular kinematics and a motion model for the target. A state augmentation is exploited that allows the proposed formulation to be considered as linear time-varying without linearizing the original nonlinear systems. Constructive observability results can then be established, leading naturally to the design of a Kalman Filter with GES error dynamics. These results also provide valuable insight on the motion planning of the vehicle. Simulation results demonstrate the good performance of the algorithm and help validate the theoretical results, as well as illustrate the necessity of a proper trajectory.**

I. Introduction

Simultaneous localization and mapping (SLAM) is the problem of navigating a vehicle in an unknown environment, by building a map of the area and using this map to deduce its location, without the need for a priori knowledge of location. It has been subject of intensive research by the community, and a myriad of approaches have arisen, varying in filtering concept and type of sensors used (see [1] and [2] for a two-part survey on this matter). Although the most studied version of the SLAM problem is what is called range-bearing SLAM, where the coordinates of measured beacons are readily available, there are versions of the problem that omit one of the two informations available, either range-only SLAM (RO-SLAM) or bearing-only SLAM (BO-SLAM). These approaches are named partially-observable, as a single noise-free observation provides only a line or surface as an estimate for the position of a beacon. This is one of the main problems in RO-SLAM, i.e., the initialization of the algorithm. The common RO-SLAM formulation has similarities with the problem of Sensor Networks (SN), in the sense that there is an agent receiving signals from a network of sensors, and, therefore, the two ideas have been used in conjunction in works such as [3] and [4], where, along with agent-to-sensor ranges, sensor-to-sensor ranges are also used, thus approximating the RO-SLAM problem to the sensor network localization problem. In that direction, the authors of [5] use the concept of multi-hop measurements in the SLAM context.

In spite of their proximity, the fields of SLAM and self-localization of sensor networks have historically been treated separately and by different fields of research, robotics and signal processing. Due to that fact, very different approaches have been taken to produce algorithms for each of these topics, from the Bayesian approach of robotics to the convex optimization-based solutions spawned by signal processing. The proliferation of (wireless) sensor network applications, including environmental monitoring, intrusion detection, search and rescue, within others, has led to a significant research interest on the development of localization techniques (see [6] and references therein for an overview of these techniques). Due to the inherent distributed computation capabilities of a sensor network, several self-localization algorithms have been developed to explore those capabilities, of which [7] is a good example as it provides an optimization algorithm that addresses both range-based and connectivity-based localization. Most algorithms rely on nonlinear optimization problems with convex relaxation techniques or on multidimensional scaling [8].

Another typical use of sensor networks is the tracking of moving objects. This is mostly known in the scientific community as the simultaneous localization and tracking problem [9] and is closely related to SLAM. It is usually formulated in a Bayesian framework [10], which brings it further closer to SLAM.

In this paper, it is proposed a fusion of all these concepts in a RO-SLAM framework. With this approach, a motion-aided mapping of the sensor network is achieved. Taking advantage of the sensor-based approach that allows the whole network to be observable without anchors (as opposed to the absolute or inertial approach that requires anchors [8]), this paper introduces a novel algorithm for RO-SLAM in sensor networks with moving object tracking (SN-SLAMMOT) that eliminates the initialization problem through the establishment of global convergence results with a tridimensional (3-D) sensor-based formulation that avoids the representation of the pose of the vehicle in the state, as it becomes deterministic and available by construction. This SN-SLAMMOT solution builds on a preliminary version that presented only RO-SLAM capabilities [11], and is grounded on the source-localization algorithm proposed in [12] and the long baseline (LBL) navigation algorithm presented in [13], as the global convergence results are achieved through similar state augmentations.

This work was supported by the Fundação para a Ciência e a Tecnologia (FCT) through ISR under LARSyS UID/EEA/50009/2013, and through IDMEC, under LAETA UID/EMS/50022/2013 projects, and by the University of Macau MYRG117(Y1-L3)-FST12-MKM project. The work of P. Lourenço was supported by the PhD Student Grant SFRH/BD/89337/2012 from FCT.

The authors are with the Institute for Systems and Robotics, Laboratory of Robotics and Systems in Engineering and Practice, Portugal. P. Batista is also with Instituto Superior Técnico, Universidade de Lisboa, Portugal. P. Oliveira is also with the Department of Mechanical Engineering, Instituto Superior Técnico, Universidade de Lisboa, Portugal. C. Silvestre is with the Department of Electrical and Computer Engineering of the Faculty of Science and Technology of the University of Macau, Macao, China, on leave from Instituto Superior Técnico, Universidade de Lisboa, Lisbon, Portugal.
{plourenco,pbatista,pjcro,cjs}@isr.ist.utl.pt

The main contributions of this paper are the design, analysis, and experimental validation of a 3-D SN-SLAMMOT algorithm that (i) has globally exponentially stable (GES) error dynamics; (ii) resorts to the exact linear and angular motion kinematics; (iii) solves a nonlinear problem with no linearizations whatsoever; and (iv) builds on the well-established linear time-varying Kalman filtering theory. Note that, although the maps and the target position provided by this filter are expressed in vehicle-centric coordinates, it is possible to obtain an inertial estimate of the map, the vehicle pose, and the target position using, for example, the algorithm proposed in [14], in which a methodology was presented to obtain inertial estimates of the pose of the vehicle and of the beacon map using only the sensor-based map. This algorithm was successfully used with other purely sensor-based SLAM filters such as [15] and [16].

Throughout the paper, the symbol $\mathbf{0}_{n\times m}$ denotes an $n\times m$ matrix of zeros (if only one subscript is present, the matrix is square), $\mathbf{I}_n$ is an identity matrix with dimension n, $\mathrm{diag}\,(\mathbf{A}_1,\ldots,\mathbf{A}_n)$ is a block diagonal matrix, and $\mathbf{1}_n$ is a $n\times 1$ vector of ones.

II. SLAM IN SENSOR NETWORKS

A. Problem statement

Consider the existence of a sensor network composed of several static nodes, or beacons, and two mobile nodes, or agents. One of the agents is a full-fledged vehicle with several sensing capabilities, such as ranging, as well as angular and linear odometry. The other agent is merely passive, i.e., it does not measure any motion-related variables and its distance to other nodes is only measured by them. This could represent a person, another vehicle in an enemy setting, within other possibilities. The sensor network distributes among its nodes the range measurements acquired by each of its nodes. Therefore, each beacon can maintain an average filter for the range from its static neighbours, thus reducing the uncertainty of that information. The vehicle is the only node with real computing capabilities, and therefore the localization of itself and the remaining network is performed in the vehicle. This renders the problem at hands a simultaneous localization and mapping/tracking problem. One advantage of looking at this in a SLAM framework is that with the regular algebraic solutions for sensor-network localization data loss is a very relevant issue as is network connectivity. With a SLAM filter, as long as certain observability conditions are fulfilled, the whole network can be localized in time.

Let $\{I\}$ be a local inertial frame and $\{B\}$ a body-fixed frame, attached to the vehicle. The pair $\left({}^I\mathbf{p}(t),\mathbf{R}(t)\right)\in\mathbb{R}^3\times \mathrm{SO}(3)$ maps frame $\{B\}$ into the inertial frame.

There are m static beacons, denoted in the inertial frame as ${}^I\mathbf{p}_i(t)\in\mathbb{R}^3$, with $i\in\mathcal{M}:=\{1,\ldots,m\}$, or in the body-fixed frame as $\mathbf{p}_i(t)\in\mathbb{R}^3$. The second agent, henceforth denominated the target, is denoted as ${}^I\mathbf{p}_T(t)\in\mathbb{R}^3$ or $\mathbf{p}_T(t)\in\mathbb{R}^3$ depending on whether it is expressed in frame $\{I\}$ or $\{B\}$.

Throughout the network, the following range measurements are available: beacon-to-beacon (B2B), denoted as $r_{ij}(t)>0$ for all $i<j$ and $i,j\in\mathcal{M}$, vehicle-to-beacon (V2B), denoted as $r_i(t)>0$ for all $i\in\mathcal{M}$, vehicle-to-target (V2T), or $r_T(t)>0$, and beacon-to-target (B2T), denoted as $r_{iT}(t)>0$ $i\in\mathcal{M}$. The vehicle has available its linear and angular velocities as expressed in its own frame, respectively $\mathbf{v}(t)\in\mathbb{R}^3$ and $\boldsymbol{\omega}(t)\in\mathbb{R}^3$. This can be seen as three-dimensional (3-D) odometry.

B. Filtering concept

The main idea behind this paper is the sensor-based approach that allows to solve one of the main nonlinearities that affects the SLAM problem: the presence of the vehicle pose in the state. In this particular formulation of SLAM, with range-only measurements, there are further nonlinearities that impair the development of filtering solutions with convergence guarantees, namely the nonlinear relation between the output (the ranges) and the state (the beacons positions). This nonlinearity can be bypassed through the use of state augmentation, as was successfully done by the authors in [12] and in the SLAM-context in [11]. In those works, the state augmentation and the sensor-based approach allowed to design systems that resemble linear time-varying systems, and therefore permit the usage of the Kalman filter with its convergence and stability properties. Following the same reasoning, this work aims at achieving global convergence and stability results in a filter for the problem described before.

a) SN-SLAM: The problem is modelled as a nonlinear dynamic system, expressed in local coordinates, fixed to the vehicle similarly to the RO-SLAM problem in [11]. In fact, if there are no agents besides the vehicle, the only difference to RO-SLAM is the presence of sensor-to-sensor ranges, and the fact that each beacon is capable of measuring distances and save them. This communication allows for the nodes without direct connectivity to a given node to have information about that node with a few timesteps of delay – allowing for multi-hop filtering when that information reaches the vehicle. Hence, the nonlinear system that encodes that part of the problem is

$$\begin{cases}\dot{\mathbf{p}}_i(t)=-\mathbf{S}\left[\boldsymbol{\omega}(t)\right]\mathbf{p}_i(t)-\mathbf{v}(t),\forall i\in\mathcal{M}\\ \dot{\mathbf{v}}(t)=\mathbf{0}\\ \mathbf{y}_V(t)=\mathbf{v}(t)\\ r_j(t)=\|\mathbf{p}_j(t)\|,\forall j\in\mathcal{M}_O\\ r_{kl}(t)=\|\mathbf{p}_k(t)-\mathbf{p}_l(t)\|,\forall k,l\in\mathcal{M}_I\end{cases}, \tag{1}$$

where $\mathbf{S}\left[\boldsymbol{\omega}(t)\right]$ is a skew-symmetric matrix that encodes the cross-product, and the linear velocity is directly measured, even though it is modelled as constant for filtering purposes. The set $\mathcal{M}_O:=\{1,\ldots,m_o\}$ represents the beacons directly observed by the vehicle (in contrast to the set $\mathcal{M}_U:=\{m_o+1,\ldots,m\}$), and the set $\mathcal{M}_I$ contains the beacons indirectly observed (note that, in general, $\mathcal{M}_O\cap\mathcal{M}_I\neq\emptyset$).

b) Tracking moving agents: Given that the second agent is passive in the network, a model must be assumed for its motion. For simplicity and to allow the use of an LBL-like structure, the constant velocity model is used in the inertial frame, resulting in

$$\begin{cases}\dfrac{d}{dt}\left(\mathbf{R}(t)\mathbf{p}_T(t)\right)={}^I\mathbf{v}_T(t)-\mathbf{R}(t)\mathbf{v}(t)\\ {}^I\dot{\mathbf{v}}_T(t)=\mathbf{0}\\ r_T(t)=\|\mathbf{p}_T(t)\|\\ r_{iT}(t)=\|\mathbf{p}_i(t)-\mathbf{p}_T(t)\|\end{cases}, \tag{2}$$

where ${}^I\mathbf{v}_T(t) \in \mathbb{R}^3$ is the velocity of the target expressed in the inertial frame, and $\mathcal{M}_T := \{1, \dots, m_T\}$ is the set of beacons whose field-of-view includes the target.

In opposition to the beacons, ranges to the target can only be used in the instant they are acquired, i.e., only the range to the target whose originating beacons are directly seen by the robot matter, as multi-hop ranges are older and cannot be easily inserted in a forward-time filter. A possibility is their use in a smoother [17] in post-processing to better recover the full trajectory of the target.

The ultimate idea behind this paper is to design a linear time-varying (LTV) system that mimics the nonlinear dynamics derived in this section, while allowing for a LTV Kalman filter to serve as the filtering engine for this problem, taking advantage of its good stability and convergence properties.

III. System design

This section presents the design of new systems that can be regarded as LTV for observability purposes, while mimicking the underlying nonlinear systems. Without loss of generality, the two systems in analysis will be treated separately, for the sake of clarity. Note that the first system is independent of the second, while the second relies on the first. For all the derivations to come, the following assumption is necessary.

Assumption 1: Any measured range from any node to any other node of the network is upper and lower bounded by some positive constants,

$$R_m < r_i(t), r_{ij}(t), r_T(t), r_{iT}(t) < R_M, \forall i, j \in \mathcal{M}, \forall t > t_0.$$

A. SN-SLAM

The system introduced in the previous section is evidently nonlinear and, as such, cannot be used directly in a Kalman filter as intended. For that reason, and given that the nonlinearity presents itself on the output equations, a strategy of state augmentation to obtain a linear relation between the system state and output is proposed. Apart from the B2B ranges, the system (1) is in every way similar to the underlying system designed in [18], and, therefore, the idea of adding the ranges to beacons to the system state proposed there will be used here as well.

In order to be able to incorporate the beacon-to-beacon ranges in this system, consider the expansion of the range from beacon i to beacon j, given by

$$r_{ij}(t) = \frac{1}{r_{ij}(t)} \left(\mathbf{p}_i^T(t)\mathbf{p}_i(t) + \mathbf{p}_j^T(t)\mathbf{p}_j(t) - 2\mathbf{p}_i^T(t)\mathbf{p}_j(t) \right). \tag{3}$$

Note that the first two parcels in (3) are in fact the square of the ranges to beacons i and j and therefore could be substituted by those quantities whenever available. However, to allow for the use of these ranges even when one or more of the corresponding beacons are not directly visible, the squared ranges are added to the state of the system, in contrast to the augmented state in [18] which consisted of the ranges. The last parcel, the dot product between the two beacons, is also nonlinear on the state of the original system (1), and therefore it is also added to the state.

To summarize all this information, the new state is $\mathbf{x}(t) := \left[\mathbf{x}_M^T(t)\ \mathbf{x}_V^T(t)\ \mathbf{x}_R^T(t)\ \mathbf{x}_D^T(t)\right]^T$, where each component is given by

$$\begin{cases} \mathbf{x}_M(t) := \{\mathbf{p}_i(t), \forall i \in \mathcal{M}\} \in \mathbb{R}^{3m} \\ \mathbf{x}_V(t) := \mathbf{v}(t) \in \mathbb{R}^3 \\ \mathbf{x}_R(t) := \{\|\mathbf{p}_i(t)\|^2, \forall i \in \mathcal{M}\} \in \mathbb{R}^m \\ \mathbf{x}_D(t) := \{\mathbf{p}_i^T(t)\mathbf{p}_j(t), \forall i, j \in \mathcal{M}, i < j\} \in \mathbb{R}^{C_2^m} \end{cases}. \tag{4}$$

The augmented system dynamics are

$$\begin{cases} \dot{\mathbf{x}}(t) = \mathbf{A}(t, \mathbf{y}_V(t))\mathbf{x}(t) \\ \mathbf{y}(t) = \mathbf{C}(t)\mathbf{x}(t) \end{cases}, \tag{5}$$

where the dynamics matrix is

$$\mathbf{A}(t) = \begin{bmatrix} \mathbf{A}_M(t) & \mathbf{A}_{MV} & \mathbf{0}_{3m\times m} & \mathbf{0}_{3m\times C_2^m} \\ \mathbf{0}_{3\times 3m} & \mathbf{0}_{3\times 3} & \mathbf{0}_{3\times m} & \mathbf{0}_{3\times C_2^m} \\ -2\mathbf{A}_{RM}(t) & \mathbf{0}_{m\times 3} & \mathbf{0}_{m\times m} & \mathbf{0}_{m\times C_2^m} \\ -\mathbf{A}_{DM}(t) & \mathbf{0}_{C_2^m\times 3} & \mathbf{0}_{C_2^m\times m} & \mathbf{0}_{C_2^m\times C_2^m} \end{bmatrix},$$

with $\mathbf{A}_M(t) := -\operatorname{diag}\left(\mathbf{S}\left[\boldsymbol{\omega}(t)\right], \dots, \mathbf{S}\left[\boldsymbol{\omega}(t)\right]\right)$, $\mathbf{A}_{MV} := \left[-\mathbf{I}_3\ \cdots\ -\mathbf{I}_3\right]^T$, $\mathbf{A}_{RM}(t) := \operatorname{diag}\left(\mathbf{y}_V^T(t), \dots, \mathbf{y}_V^T(t)\right)$, and $\mathbf{A}_{DM}(t)$ is the matrix that encodes all the possible combinations of two beacons, such that $\frac{d}{dt}\mathbf{p}_i(t)^T\mathbf{p}_j(t) = -\mathbf{y}_V^T(t)\left(\mathbf{p}_i(t) + \mathbf{p}_j(t)\right)$ for all $i < j$, $i, j \in \mathcal{M}$. The output matrix is

$$\mathbf{C}(t) = \begin{bmatrix} \mathbf{0}_{3\times 3m} & \mathbf{I}_3 & \mathbf{0}_{3\times m_o} & \mathbf{0}_{3\times m_u} & \mathbf{0}_{3\times C_2^m} \\ \mathbf{0}_{m\times 3m} & \mathbf{0}_{m\times 3} & \mathbf{C}_R(t) & \mathbf{0}_{m_o\times m_u} & \mathbf{0}_{3\times C_2^m} \\ \mathbf{0}_{C_2^{m_i}\times 3m} & \mathbf{0}_{C_2^{m_i}\times 3} & \mathbf{C}_{DR}(t) & \mathbf{0}_{C_2^{m_i}\times m_u} & -2\mathbf{C}_D(t) \end{bmatrix},$$

where the first m_o range states were separated from the m_u non-visible ones. Its components are $\mathbf{C}_R(t) := \operatorname{diag}\left(r_1^{-1}(t), \dots, r_{m_o}^{-1}(t)\right)$, $\mathbf{C}_D(t) := \left[\operatorname{diag}\left(r_{12}^{-1}(t), \dots, r_{(m_i-1)m_i}^{-1}(t)\right)\ \mathbf{0}_{C_2^{m_i}\times(C_2^m - C_2^{m_i})}\right]$, and $\mathbf{C}_{DR}(t)$ is the matrix that encodes all the possible combinations of two observed beacons, such that $r_{ij}(t) = r_{ij}^{-1}(t)\left(x_{R_i} + x_{R_j} - 2x_{D_{ij}}\right)$ for all $i < j$, $i, j \in \mathcal{M}_I$.

B. Tracking

The target tracking part of the system is more complicated to tackle than the previous one. Let $\mathbf{z}_{T_P}(t) = \mathbf{R}(t)\mathbf{p}_T(t)$ and $\mathbf{z}_{T_V}(t) := {}^I\mathbf{v}_T(t)$ be its states. Consider the two types of ranges to the target that the vehicle has access to: vehicle-to-target and beacon-to-target. Following the reasoning in [13], a series of new states are added to yield a linear-like structure to the output-state relation. Take, for example, the vehicle-to-target range, $r_T(t) = \|\mathbf{z}_{T_P}(t)\|$. If it is added to the state, the output will be linear-like with respect to the state, with dynamics given by

$$\frac{d}{dt}(r_T^2(t)) = 2\mathbf{z}_{T_V}^T(t)\mathbf{z}_{T_P} - 2{}^I\mathbf{v}^T(t)\mathbf{z}_{T_P}(t).$$

The first parcel can then be added to a new state, $z_{T_{VP}}(t) := \mathbf{z}_{T_V}^T(t)\mathbf{z}_{T_P}$, yielding

$$\dot{z}_{T_{VP}}(t) := \mathbf{z}_{T_V}^T(t)\mathbf{z}_{T_V}(t) - {}^I\mathbf{v}^T(t)\mathbf{z}_{T_V}(t),$$

and denoting the first parcel as $z_{T_{VV}}(t) := \mathbf{z}_{T_V}^T(t)\mathbf{z}_{T_V}(t)$, its derivative is

$$\dot{z}_{T_{VV}}(t) = 0.$$

To tackle the inclusion of the beacon-to-target ranges in the system, consider its expansion as in (3),

$$\begin{aligned} r_{iT}^2(t) &= \|\mathbf{R}(t)\mathbf{p}_i(t) - \mathbf{z}_{T_P}(t)\|^2 \\ &= x_{R_i}(t) + z_{T_R}(t) - 2\mathbf{z}_{T_P}^T(t)\mathbf{R}(t)\mathbf{p}_i(t), \end{aligned}$$

where $x_{R_i}(t)$ and $z_{T_R}(t)$ are replacing the corresponding squared ranges. The last parcel can then be added as a new state, $z_{T_{P_i}}(t)$, with dynamics given by

$$\dot{z}_{T_{P_i}}(t) = \mathbf{z}_{T_V}^T(t)\mathbf{R}(t)\mathbf{p}_i(t) - {}^I\mathbf{v}^T(t)\left(\mathbf{R}(t)\mathbf{p}_i(t) + \mathbf{z}_{T_P}(t)\right).$$

Once again, the first nonlinear parcel is replaced by a new state, $z_{T_{V_i}}(t)$, whose derivative is

$$\dot{z}_{T_{V_i}}(t) = -{}^I\mathbf{v}^T(t)\mathbf{z}_{T_V}(t).$$

The quantities introduced here can then be stacked in the target state,

$$\mathbf{z}_T(t) = \left[\mathbf{z}_{T_P}^T(t)\, \mathbf{z}_{T_V}^T(t)\, z_{T_R}(t)\, z_{T_{VP}}(t)\, z_{T_{VV}}(t)\, \mathbf{z}_{T_{PM}}(t)\, \mathbf{z}_{T_{VM}}(t)\right]^T,$$

where $\mathbf{z}_{T_{PM}}(t) \in \mathbb{R}^m$ and $\mathbf{z}_{T_{VM}}(t) \in \mathbb{R}^m$ are the stacking of all the $z_{T_{Pi}}(t)$ and $z_{T_{Vi}}(t)$ respectively.

It must be noted that although present in all the expressions in this subsection, the rotation matrix is not observed nor estimated. To avoid this issue, consider the state $\mathbf{x}_T(t) := \operatorname{diag}\left(\mathbf{R}^T(t), \mathbf{R}^T(t), 1, 1, 1, \mathbf{I}_m, \mathbf{I}_m\right)\mathbf{z}_T(t)$. The new augmented system that can be joined with (5) is

$$\begin{cases} \dot{\mathbf{x}}_T(t) = \mathbf{A}_T(t)\mathbf{x}_T(t) + \mathbf{A}_{TB}(t)\mathbf{x}(t) \\ \mathbf{y}_T(t) = \mathbf{C}_T(t)\mathbf{x}_T(t) + \mathbf{C}_{TB}(t)\mathbf{x}(t) \end{cases}, \tag{6}$$

where the dynamics matrix is composed of

$$\mathbf{A}_T(t) = \begin{bmatrix} -\mathbf{S}\left[\boldsymbol{\omega}(t)\right] & \mathbf{I}_3 & \mathbf{0}_{3\times1} & \mathbf{0}_{3\times1} & \mathbf{0}_{3\times1} & \mathbf{0}_{3\times m} & \mathbf{0}_{3\times m} \\ \mathbf{0}_{3\times3} & -\mathbf{S}\left[\boldsymbol{\omega}(t)\right] & \mathbf{0}_{3\times1} & \mathbf{0}_{3\times1} & \mathbf{0}_{3\times1} & \mathbf{0}_{3\times m} & \mathbf{0}_{3\times m} \\ -2\mathbf{y}_V^T & \mathbf{0}_{1\times3} & 0 & 2 & 0 & \mathbf{0}_{3\times m} & \mathbf{0}_{3\times m} \\ \mathbf{0}_{1\times3} & -\mathbf{y}_V^T & 0 & 0 & 1 & \mathbf{0}_{3\times m} & \mathbf{0}_{3\times m} \\ \mathbf{0}_{1\times3} & \mathbf{0}_{1\times3} & 0 & 0 & 0 & \mathbf{0}_{1\times m} & \mathbf{0}_{1\times m} \\ -\mathbf{1}_m\mathbf{y}_V^T & \mathbf{0}_{m\times3} & \mathbf{0}_{m\times1} & \mathbf{0}_{m\times1} & \mathbf{0}_{m\times1} & \mathbf{0}_{m\times m} & \mathbf{I}_m \\ \mathbf{0}_{m\times3} & -\mathbf{1}_m\mathbf{y}_V^T & \mathbf{0}_{m\times1} & \mathbf{0}_{m\times1} & \mathbf{0}_{m\times1} & \mathbf{0}_{m\times m} & \mathbf{0}_{m\times m} \end{bmatrix}$$

and

$$\mathbf{A}_{TB}(t) = \begin{bmatrix} \mathbf{0}_{3\times3m} & -\mathbf{I}_3 & \mathbf{0}_{3\times m} & \mathbf{0}_{3\times C_2^m} \\ \mathbf{0}_{3\times3m} & \mathbf{0}_{3\times3} & \mathbf{0}_{3\times m} & \mathbf{0}_{3\times C_2^m} \\ \mathbf{0}_{1\times3m} & \mathbf{0}_{1\times3} & \mathbf{0}_{1\times m} & \mathbf{0}_{1\times C_2^m} \\ \mathbf{0}_{1\times3m} & \mathbf{0}_{1\times3} & \mathbf{0}_{1\times m} & \mathbf{0}_{1\times C_2^m} \\ \mathbf{0}_{1\times3m} & \mathbf{0}_{1\times3} & \mathbf{0}_{1\times m} & \mathbf{0}_{1\times C_2^m} \\ -\mathbf{A}_{RM}(t) & \mathbf{0}_{m\times3} & \mathbf{0}_{m\times m} & \mathbf{0}_{m\times C_2^m} \\ \mathbf{0}_{1\times3m} & \mathbf{0}_{1\times3} & \mathbf{0}_{1\times m} & \mathbf{0}_{1\times C_2^m} \end{bmatrix}.$$

Finally, the output matrices of this part of the system are

$$\mathbf{C}_T(t) = \begin{bmatrix} \mathbf{0}_{1\times3} & \mathbf{0}_{1\times3} & r_T^{-1}(t) & 0 & 0 & \mathbf{0}_{1\times m} & \mathbf{0}_{1\times m} \\ \mathbf{0}_{m_T\times3} & \mathbf{0}_{m_T\times3} & \mathbf{C}_{T_R}(t) & 0 & 0 & -2\mathbf{C}_{T_P}(t) & \mathbf{0}_{1\times m} \end{bmatrix}$$

and

$$\mathbf{C}_{TB}(t) = \begin{bmatrix} \mathbf{0}_{1\times3m} & \mathbf{0}_{1\times3} & \mathbf{0}_{1\times m} & \mathbf{0}_{1\times C_2^m} \\ \mathbf{0}_{m_T\times3m} & \mathbf{0}_{m_T\times3} & \mathbf{C}_{T_P}(t) & \mathbf{0}_{m_T\times C_2^m} \end{bmatrix},$$

where $\mathbf{C}_{T_R}(t) = \begin{bmatrix} r_{1T}^{-1} & \cdots & r_{m_TT}^{-1} \end{bmatrix}^T$ and $\mathbf{C}_{T_P}(t) = \begin{bmatrix} \operatorname{diag}\left(r_{1T}^{-1}, \ldots, r_{m_TT}^{-1}\right) & \mathbf{0}_{m_T\times(m-m_T)c} \end{bmatrix}$.

These new systems, that mimic the dynamics of (1) and (2), are still nonlinear in form. In fact, the time dependence of the dynamics and output matrices hides the dependence on the system output through the linear velocity of the vehicle and the measured ranges, two known signals. However, for that reason they are considered linear time-varying systems for observability purposes. Furthermore, the algebraic constraints that helped define $\mathbf{x}(t)$ and $\mathbf{x}_T(t)$ are not imposed anywhere in the system dynamics.

Note that in the systems designed here, it is assumed that the first m_o beacons are directly observed, the first m_i are within the field-of-view of each other, and the first m_T can measure ranges to the target. In practice, any beacon can be in either sets.

C. Observability analysis

The augmented system that does not include the dynamics of the target is, as mentioned, very similar to the augmented system derived in [11]. In fact, the inclusion of the beacon-to-beacon ranges does not lighten the observability requirements established therein. Therefore, this first part of the observability analysis is quite straightforward.

In this analysis, the invisible beacons, ranges, and dot products are removed from the states, as they cannot be observable. Therefore, the set $\mathcal{M}_U$ is considered to be empty and the sets $\mathcal{M}_I$ and $\mathcal{M}_T$ are contained in $\mathcal{M}_O$.

Theorem 1: Consider the system (5) and let $\mathcal{T} := [t_0, t_f]$. If there exist three instants $\{t_1, t_2, t_3\} \in \mathcal{T}$ such that the linear velocity of the vehicle expressed in the inertial frame is linearly independent in those instants, i.e., $\det\left(\begin{bmatrix} {}^I\mathbf{v}(t_1) & {}^I\mathbf{v}(t_2) & {}^I\mathbf{v}(t_3) \end{bmatrix}\right) \neq 0$, then the system is observable in the sense that, given the system output $\{\mathbf{y}(t),\, t \in \mathcal{T}\}$, the initial condition $\mathbf{z}(t_0)$ is uniquely defined.

The following theorem is necessary to establish a clear relation between the augmented system (5) that mimics the nonlinear dynamics with the actual nonlinear system (1).

Theorem 2: Consider the LTV system (5) and the original nonlinear system (1). If the conditions of Theorem 1 hold, then the state of the original nonlinear system and that of the LTV system are the same and uniquely defined, provided that the invisible beacons are discarded. Furthermore the constraints expressed by (4) become naturally imposed by the dynamics.

The tracking of a target with unknown motion in a SLAM framework is more complex than simple mapping, and therefore it will impose stronger requirements on the motion of the vehicle. The following theorem addresses this issue, but requires the definition of two functions of the linear velocity, $\boldsymbol{\mathcal{V}}^{[0]}(t, t_0) = {}^I\mathbf{v}(t) - {}^I\mathbf{v}(t_0)$ and $\boldsymbol{\mathcal{V}}^{[1]}(t, t_0) = \int_{t_0}^{t} {}^I\mathbf{v}(\tau)\mathrm{d}\tau + (t - t_0){}^I\mathbf{v}(t)$, each composed of three components $\mathcal{V}_1^{[.]}(t, t_0)$, $\mathcal{V}_2^{[.]}(t, t_0)$, and $\mathcal{V}_3^{[.]}(t, t_0)$.

To simplify the analysis, the set $\mathcal{M}_I$ is assumed to be empty, i.e., there are no B2B ranges.

Theorem 3: The systems (5) and (6) are observable if the conditions of Theorem 1 hold, if the functions $\mathcal{V}_1^{[0]}(t, t_0)$, $\mathcal{V}_2^{[0]}(t, t_0)$, $\mathcal{V}_3^{[0]}(t, t_0)$, $\mathcal{V}_1^{[1]}(t, t_0)$, $\mathcal{V}_2^{[1]}(t, t_0)$, and $\mathcal{V}_3^{[1]}(t, t_0)$ are linearly independent in $\mathcal{T}$ and at least one B2T range is available three times in $\mathcal{T}$. If there are no B2T ranges, the $\mathcal{V}$ functions must also be linearly independent to $(t - t_0)$.

Theorems 1 and 3 established conditions in which reduced versions of the augmented systems (5) and (6) are observable. As the discarded states are not observable, and do not influence the non discarded ones, these results also apply to the augmented systems even when there are non-visible beacons. However, this does not immediately establish an equivalence between the augmented systems and the original nonlinear ones. Furthermore, the state relations stated in 4 and those described in subsection III-B are not imposed.

Theorem 2 addressed the first constraints, and the following result will address the latter.

Theorem 4: If the conditions of Theorem 3 hold, the systems (2) and (6) are equivalent, when discarding the non-visible beacons and respective ranges, and:

(i) the state of the original nonlinear system and that of the LTV system are the same and uniquely defined, provided that the invisible beacons are discarded. Furthermore the constraints described in subsection III-B become naturally imposed by the dynamics; and

(ii) a state observer with uniformly globally exponentially stable error dynamics for the LTV system is also a state observer for the underlying nonlinear system, and the estimation error converges exponentially fast for all initial conditions.

Remark 1: Due to space constraints, the proofs of the results of this paper are omitted. The reader is referred to [12] and [11] for similar proofs for slightly different dynamics.

IV. Filter Design

The previous results have established the ground to the design of a GES observer, using a linear time-varying Kalman filter, which, to assure the GES nature of the estimation error dynamics, requires the pair $(\mathbf{A}_F(t), \mathbf{C}_F(t))$ to be uniformly completely observable. This can be shown using the Lyapunov function $V(t, \tilde{\mathbf{x}}_F) = \tilde{\mathbf{x}}_F^T(t)\mathbf{P}^{-1}(t)\tilde{\mathbf{x}}_F(t)$, where $\tilde{\mathbf{x}}_F(t)$ is the observer error and $\mathbf{P}(t)$ is the error covariance and demonstrating that it respects all the conditions of [19, Theorem 8.5] for global exponential stability. The steps taken are similar to [19, Example 8.5] and include showing that $\mathbf{P}^{-1}(t)$ is positive definite using several results of [20]. This last theorem addresses the uniform complete observability of the pair $(\mathbf{A}(t), \mathbf{C})$. However, an additional assumption on the linear velocity of the vehicle is required, as well as the definition of $\boldsymbol{\mathcal{V}}(\tau, t) := \left[\boldsymbol{\mathcal{V}}^{[0]}(\tau, t)\ \boldsymbol{\mathcal{V}}^{[1]}(\tau, t)\right]^T$.

Assumption 2: The norm of the linear velocity of the vehicle in the inertial frame $\{I\}$ is always bounded, i.e.,

$$\underset{t \geq t_0}{\forall} \quad \underset{V_M > 0}{\exists} : \quad \|^I\mathbf{v}(t)\| \leq V_M.$$

Although imposing bounds on the linear velocity, this assumption is still a mild one, as it is physically impossible to reach arbitrarily large speeds. Moreover, the value of V_M is not required for the filter design.

Theorem 5: The pair $(\mathbf{A}(t), \mathbf{C})$ is uniformly completely observable if Assumption 2 is true and there exist $\delta > 0$ and $\alpha^* > 0$ such that, for all $t \geq t_0$, it is possible to choose a set of instants $\{t_1, t_2, t_3, t_4, t_5, t_6, t_7\} \in \mathcal{T}_\delta$, with $\mathcal{T}_\delta := [t, t+\delta]$, for which the linear velocity of the vehicle in the inertial frame respects

$$\left|\det\left[\boldsymbol{\mathcal{V}}(t_1, t)\ \cdots\ \boldsymbol{\mathcal{V}}(t_6, t)\right]\right| \geq \alpha^*$$

and there is a B2T range available, or if there is not,

$$\left|\det\begin{bmatrix}\boldsymbol{\mathcal{V}}(t_1, t) & \cdots & \boldsymbol{\mathcal{V}}(t_7, t) \\ (t_1 - t) & \cdots & (t_7 - t)\end{bmatrix}\right| \geq \alpha^*.$$

The theoretical results of this paper were established in a deterministic setting, and thus the presence of measurement noise raises the need for a filtering solution. Hence, a Kalman filter follows naturally for the augmented nonlinear systems (5) and (6), in a discrete-time framework, obtained using the forward Euler discretization as in [18]. The algorithm is therefore the standard discrete-time LTV Kalman filter [17].

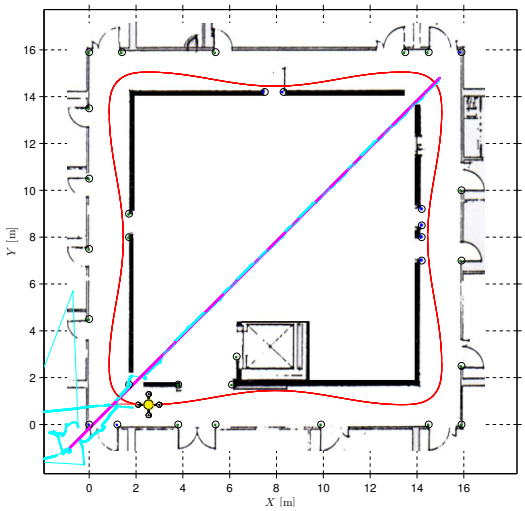

Fig. 1. Picture of the estimated map rotated and translated using the true transformation, with 2σ ellipsoids, and the path of the target, both real and estimated. Non-visible beacons in blue; Visible beacons in green; Vehicle path in red; Real target path in magenta; Estimated target path in cyan.

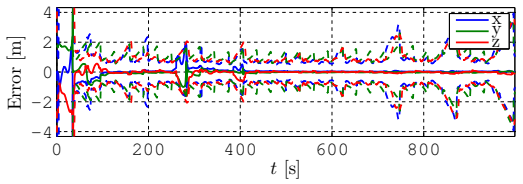

(a) Position error.

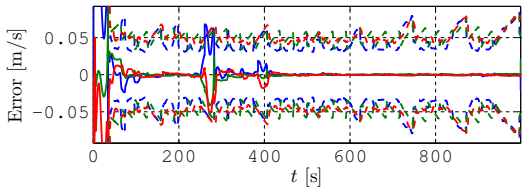

(b) Velocity error.

Fig. 2. The estimation error and 3σ uncertainty bounds of the target position and velocity when it follows a straight line. Solid lines indicate the estimation error for each coordinate and dashed lines the uncertainty bounds.

V. Simulation Results

This section details the simulations performed to validate the algorithm proposed in this paper and assess its performance. The results of a typical run in the simulated environment are presented and discussed. The chosen environment is similar to the fifth floor of the North Tower at IST, although it was modified to include a large open space. It consists of a 16 m by 16 m by 3 m corridor. 36 beacons were put in notable places such as corners and doors, with random heights. All the measurements are assumed to be perturbed by zero-mean Gaussian white noise, with standard deviations of $\sigma_\omega = 0.05\ ^\circ/\text{s}$ for the angular rates, $\sigma_v = 0.03$ m/s for the linear velocity, and $\sigma_r = 0.03$ m for the ranges. The trajectory of the vehicle is depicted in red in Fig. 1, and was designed to meet the observability requirements. The results of a simulation without a target to track are very similar to the simulation and experimental results detailed in [18]. Comparison with these results shows that the uncertainty does not grow as much when the beacons are not observed,

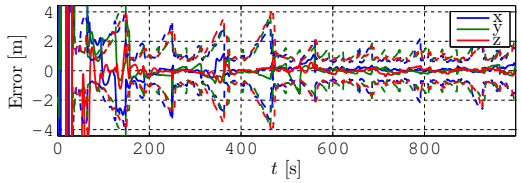

(a) Position error.

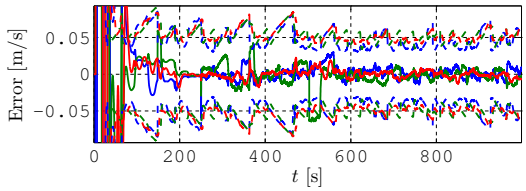

(b) Velocity error.

Fig. 3. The estimation error and 3σ uncertainty bounds of the target position and velocity when it follows a random trajectory.

although its lowest value when the estimation converges is very near the achieved with the simple RO-SLAM algorithm (10 cm). The next figures depict the results of two different simulations of target tracking. In the first, the target starts in the bottom right and is stopped for the first 250 seconds. Then it accelerates until reaching constant velocity while describing a straight line as depicted in Fig. 1. This trajectory was chosen because it is the only one that respects the constant velocity model. The results of this simulation are presented in Fig. 2. Note that the algorithm takes around 100 seconds to converge, but when it does, the error is kept very low until the target starts moving and the error grows, just to converge again when the algorithm tends to the new velocity of the target. The 3σ uncertainty is consistent with the errors, except for a few moments when the target starts moving. To illustrate a case in which the constant velocity model is not correct, in the second simulation, the target is placed randomly in the environment and, after 250 seconds stopped, starts moving in a random walk (${}^I\mathbf{v}_T(t_{k+1}) = {}^I\mathbf{v}_T(t_k) + \mathbf{u}(t_k)$ where $\mathbf{u}(t_k)$ is zero-mean Gaussian white noise), while restricted to the confines of the environment. The results of a typical run are shown in Fig. 3. Once again, the theoretical convergence properties are confirmed by the results, as, albeit being initialized at the origin of the body-fixed frame, the estimation converges fairly fast. Even when the vehicle starts moving, the filter accompanies the motion and the error does not increase significantly except when the velocity is inverted at around 500 seconds into the run.

VI. Conclusions

This paper presented a novel sensor-based range-only simultaneous localization and mapping in sensor networks filter with moving target tracking. The filter is shown to have globally exponentially stable error dynamics, through state augmentation of two nonlinear systems, which, along with the disposal of the non-visible beacons, enabled regarding the resulting system as linear time-varying. The work focused on the observability analysis of the resulting system, providing theoretical observability guarantees, and equivalence between the systems used in each step of the analysis. The theoretical results include the derivation of sufficient conditions for observability, stability and convergence of the algorithm, establishing a constructive basis for trajectory design. These results were followed by the design of a Kalman filter with globally exponentially stable error dynamics. Simulations allowed the validation of the results while demonstrating the need for a properly designed trajectory. As for future work, the investigation of necessary conditions for observability and the experimental validation of the proposed algorithm the two main courses of action.

References

[1] H. Durrant-Whyte and T. Bailey, "Simultaneous Localisation and Mapping (SLAM): Part I The Essential Algorithms," *IEEE Robotics & Automation Magazine*, vol. 13, no. 2, pp. 99–110, 2006.

[2] T. Bailey and H. Durrant-Whyte, "Simultaneous localization and mapping (SLAM): Part II," *IEEE Robotics & Automation Magazine*, vol. 13, no. 3, pp. 108–117, 2006.

[3] J. Djugash and S. Singh, "Motion-aided network SLAM with range," *The International Journal of Robotics Research*, vol. 31, no. 5, pp. 604–625, 2012.

[4] A. Torres-González, J.-D. Dios, and A. Ollero, "Efficient robot-sensor network distributed seif range-only slam," in *Robotics and Automation (ICRA), 2014 IEEE International Conference on*, May 2014, pp. 1319–1326.

[5] A. Torres-González, J. M. de Dios, and A. Ollero, "Exploiting multi-hop inter-beacon measurements in ro-slam," *Procedia Computer Science*, vol. 32, no. 0, pp. 1101 – 1107, 2014, the 5th International Conference on Ambient Systems, Networks and Technologies (ANT-2014), the 4th International Conference on Sustainable Energy Information Technology (SEIT-2014).

[6] G. Mao, B. Fidan, and B. D. Anderson, "Wireless sensor network localization techniques," *Computer Networks*, vol. 51, no. 10, pp. 2529 – 2553, 2007.

[7] Q. Shi, C. He, H. Chen, and L. Jiang, "Distributed Wireless Sensor Network Localization Via Sequential Greedy Optimization Algorithm," *IEEE Transactions on Signal Processing*, vol. 58, no. 6, pp. 3328–3340, June 2010.

[8] J. N. Ash and R. L. Moses, "Self-localization of sensor networks," in *Handbook on Array Processing and Sensor Networks*, ser. Adaptive and Cognitive Dynamic Systems: Signal Processing, Learning, Communications and Control, S. Haykin and K. Liu, Eds. Wiley, 2010.

[9] C.-C. Wang, C. Thorpe, S. Thrun, M. Hebert, and H. Durrant-Whyte, "Simultaneous localization, mapping and moving object tracking," *The International Journal of Robotics Research*, vol. 26, no. 9, pp. 889–916, 2007.

[10] C. Taylor, A. Rahimi, J. Bachrach, H. Shrobe, and A. Grue, "Simultaneous localization, calibration, and tracking in an ad hoc sensor network," in *Proc. of the 5th International Conference on Information Processing in Sensor Networks*. ACM, 2006, pp. 27–33.

[11] P. Lourenço, B. J. Guerreiro, P. Batista, P. Oliveira, C. Silvestre, and C. L. P. Chen, "Sensor-based Globally Exponentially Stable Range-Only Simultaneous Localization and Mapping," *Robotics and Autonomous Systems*, vol. 68, pp. 72–85.

[12] P. Batista, C. Silvestre, and P. Oliveira, "Single range aided navigation and source localization: Observability and filter design," *Systems & Control Letters*, vol. 60, no. 8, pp. 665–673, 2011.

[13] P. Batista, C. Silvestre, and P. Oliveira, "Sensor-based Long Baseline Navigation: observability analysis and filter design," *Asian Journal of Control*, vol. 16, no. 4, pp. 974–994, July 2014.

[14] P. Lourenço, B. J. Guerreiro, P. Batista, P. Oliveira, and C. Silvestre, "3-D Inertial Trajectory and Map Online Estimation: Building on a GAS Sensor-based SLAM filter," in *Proc. of the 2013 European Control Conference*, Zurich, Switzerland, July 2013, pp. 4214–4219.

[15] ——, "Preliminary Results on Globally Asymptotically Stable Simultaneous Localization and Mapping in 3-D," in *Proc. of the 2013 American Control Conference*, Washington D.C., USA, June 2013, pp. 3093–3098.

[16] B. J. Guerreiro, P. Batista, C. Silvestre, and P. Oliveira, "Globally Asymptotically Stable Sensor-based Simultaneous Localization and Mapping," *IEEE Transactions on Robotics*, vol. 29, no. 6, pp. 1380–1395, December 2013.

[17] A. Gelb, *Applied Optimal Estimation*. MIT Press, 1974.

[18] P. Lourenço, P. Batista, P. Oliveira, C. Silvestre, and C. L. P. Chen, "Sensor-based Globally Asymptotically Stable Range-Only Simultaneous Localization and Mapping," in *Proc. of the 52nd IEEE Conference on Decision and Control*, Florence, Italy, December 2013, pp. 5692–5697.

[19] H. Khalil, *Nonlinear Systems*, 3rd ed. Prentice Hall, 2002.

[20] B. D. O. Anderson, "Stability properties of Kalman-Bucy filters," *Journal of the Franklin Institute*, vol. 291, no. 2, pp. 137–144, 1971.